Acta Cryst. (1989). A**45**, 645-654

Helical Diffraction. I. The Paracrystalline Helix and Disorder Analysis

BY C. R. WORTHINGTON

Departments of Biological Sciences and Physics, Carnegie-Mellon University, Pittsburgh, PA 15213, *USA*

AND G. F. ELLIOTT*

*Biophysics Group, The Open University Oxford Research Unit, Foxcombe Hall, Berkeley Road, Boars Hill, Oxford OX*1 5*HR, England*

(*Received* 21 *November* 1988; *accepted* 26 *April* 1989)

Abstract

In a new approach to helical diffraction a helix generating function is defined, and thence an expression for the autocorrelation function (a.c.f.) for a helix is obtained. The Fourier transform of this a.c.f. gives a new expression for the diffracted intensity, which is shown to be equivalent formally to the classical expression of Cochran, Crick & Vand [*Acta Cryst.* (1952), **5**, 581-586] and A. R. Stokes (unpublished). The new expression allows straightforward examination of the effects of helical disorders on the diffracted intensity. The thermal and paracrystalline effects of disorders with cylindrical symmetry are shown, and examples are given from the diffraction of a model of the actin helix. The general case, disorder with no symmetry, is derived and the effects of axial and radial disorder, separately and together, are computed, again for the model actin helix. Translational disorder is also included, and its effects are explained. The new results are compared with existing accounts of the effects of helical disorders on fibre diffraction.

Introduction

Our interest in helical diffraction derives from unsolved problems of biological structure and function. The Fourier transform for a helical array of atoms or molecules was derived by Cochran, Crick & Vand (1952) and by Stokes (unpublished). This formulation is well known and can be found in several textbooks (*e.g.* James, 1962; Vainshtein, 1966). Our objective here is to obtain a reformulation which will allow the inclusion of disorder. In particular, we consider the case of paracrystalline disorder as defined by Hosemann & Bagchi (1962).

Biological systems are generally non-crystalline and contain a certain degree of disorder. A current example is the diffuse scattering from one-dimensional multi-layered membrane systems. In the special case of nerve myelin, the problem of the diffuse scatter due to positional disorder has been solved (Worthington, 1986). In the nerve myelin study, the basic approach was the use of autocorrelation functions in real space to obtain the diffraction formulas. In this paper our first task is to obtain an expression for the autocorrelation function (a.c.f.) of a helical array of atoms with no disorder. It will be shown that this kind of analysis can then be used to treat the cases of thermal and paracrystalline disorder. Before we start our analysis of helical diffraction it is useful to review the a.c.f. formulas and their Fourier transforms for one-dimensional systems.

Review of one-dimensional systems

An account of diffraction theory applied to one-dimensional membrane-type systems has been given by Worthington (1987). Our summary here is from the point of view of disorder problems although we retain the notation used in previous studies.

The one-dimensional unit cell has electron density $t(x)$ and width d. We use the notation: $t(x) \Leftrightarrow T(X)$, where $t(x)$ and $T(X)$ are a Fourier-transform pair and x, X are real- and reciprocal-space coordinates. The a.c.f. of the electron density $t(x)$ is denoted $j(x)$ and is defined as

$$j(x) = t(x) * t(-x), \tag{1}$$

where $*$ is the convolution symbol. The a.c.f. has width $2d$. The Fourier transform of $j(x)$ is $J(X)$, where $j(x) \Leftrightarrow J(X)$ and $J(X) = |T(X)|^2$.

When more than one unit cell is considered, the configuration of the lattice enters into the calculation of the a.c.f. of the assembly. The lattice generating function is denoted $\psi(x)$: the a.c.f. of the lattice is denoted $l(x)$ and is defined as

$$l(x) = \psi(x) * \psi(-x). \tag{2}$$

The Fourier transform of the a.c.f. $l(x)$ is $L(X)$, where $l(x) \Leftrightarrow L(X)$. In diffraction theory (James, 1962) the Fourier transform $L(X)$ is called the interference function of the lattice.

The a.c.f. of the assembly is denoted $p(x)$: the symbol p corresponds to the Patterson function of

* Author to whom reprint requests should be addressed.

0108-7673/89/090645-10$03.00

X-ray crystallography. The diffracted intensity $I(X)$ of the assembly is the Fourier transform of the a.c.f. $p(x)$, where $p(x) \Leftrightarrow I(X)$. The a.c.f. of the assembly, $p(x)$, is given by

$$p(x) = j(x) * l(x), \tag{3}$$

and the diffracted intensity $I(X)$ is simply expressed as

$$I(X) = J(X)L(X). \tag{4}$$

The a.c.f. of the one-dimensional lattice is readily obtained when the form of the lattice-generating function $\psi(x)$ is known. We consider three special lattices with well defined lattice-generating functions.

(1) *No disorder*

This perfect lattice contains N lattice points which are a distance d apart. The lattice-generating function $\psi(x)$ for this lattice is given by

$$\psi(x) = \sum_{j=0}^{j=N-1} \delta(x - jd), \tag{5}$$

where $\psi(x)$ is a sum of delta functions. The a.c.f. $l(x)$ for this lattice is expressed in series form as

$$l(x) = N\delta(x-0) + \sum_{m=1}^{m=N-1} (N-m)\delta(x \pm md), \tag{6}$$

where m is an integer. The Fourier transform $L(X)$ of $l(x)$ is given by

$$L(X) = N + 2 \sum_{m=1}^{m=N-1} (N-m) \cos 2\pi m \, dX. \tag{7}$$

This expression for the interference function for a perfect one-dimensional lattice has been given by James (1962) and Vainshtein (1966), although it is usually expressed in a different form first derived by von Laue.

(2) *Thermal disorder*

In this case the lattice points have thermal disorder: it is convenient to assume that the disorder about each lattice point is Gaussian and is represented by $g(x)$, where

$$g(x) = (1/w) \exp[-\pi(x/w)^2], \tag{8}$$

and where w is the integral width of $g(x)$. The Fourier transform of $g(x)$ is $G(X)$ and is given by

$$G(X) = \exp[-\pi(wX)^2]. \tag{9}$$

It is convenient to use the following convolution notation (Hosemann & Bagchi, 1962). The n-fold convolution of the Gaussian function $g(x)$ is $\tilde{g}^n(x)$ and is defined as

$$\tilde{g}^n(x) = g(x) * g(x) * \ldots * g(x), \tag{10}$$

where the r.h.s. of (10) contains n convolutions. The Fourier transform of $\tilde{g}^n(x)$ is $G^n(X)$, where $\tilde{g}^n(x) \Leftrightarrow G^n(X)$ and where $G^n(X) = \exp[-\pi n(wX)^2]$.

The a.c.f. of the thermally disordered lattice is denoted $l_{td}(x)$. The expression for $l_{td}(x)$ has a certain simplicity in that the contribution between the nth neighbors involves the constant factor $\tilde{g}^2(x)$ for all values of n. Thus, the a.c.f. $l_{td}(x)$ is given by

$$l_{td}(x) = N\delta(x-0) + \sum_{m=1}^{m=N-1} (N-m)\delta(x \pm md) * \tilde{g}^2(x). \tag{11}$$

In the case of thermal disorder, the conventional notation $M = \pi(wX)^2$ is adopted, so that the Fourier transform of $\tilde{g}^2(x)$ is simply $\exp(-2M)$. The Fourier transform $L_{td}(X)$ of $l_{td}(x)$ is then given by

$$L_{td}(X) = N + 2\exp(-2M) \times \sum_{m=1}^{m=N-1} (N-m) \cos 2\pi m \, dX. \tag{12}$$

It is usual, however, to express the interference function $L_{td}(X)$ in two parts: the diffuse intensity and the intensity due to the interference function for the average lattice. Comparison with (7) shows that $L_{td}(X)$ may be written in the conventional form

$$L_{td}(X) = N(1 - e^{-2M}) + e^{-2M}L(X). \tag{13}$$

This formula was first derived by Debye in 1913 using a different approach (see James, 1962).

(3) *Paracrystalline disorder*

In this case the lattice points have paracrystalline disorder as defined by Hosemann & Bagchi (1962). Each lattice point is generated by a Gaussian probability $q(x)$ which has the same form as $g(x)$ in (8) but with the appropriate integral width w. Consequently, the lattice points have only an average separation distance d. The a.c.f of this lattice is denoted $l_{pd}(x)$ and it has the property that the contribution between mth neighbors involves the factor $\tilde{q}^m(x)$. The a.c.f. $l_{pd}(x)$ is then given by

$$l_{pd}(x) = N\delta(x-0) + \sum_{m=1}^{m=N-1} (N-m)\delta(x \pm md) * \tilde{q}^m(x). \tag{14}$$

Since the Fourier transform of $\tilde{q}^m(x)$ is $Q^m(X)$, the Fourier transform $L_{pd}(X)$ of the paracrystalline lattice can be expressed as

$$L_{pd}(X) = N + 2 \sum_{m=1}^{m=N-1} (N-m)Q^m(X) \cos 2\pi m \, dX. \tag{15}$$

Note that the interference functions for the three lattices have the same form except for the inclusion of the Gaussian transform: in the perfect lattice, the

transform is unity; in the thermal case, it is a constant factor e^{-2M}; in the paracrystalline case, the factor $Q^m(X)$ is contained within the summation part of (15).

The paracrystalline disorder parameters are usually expressed in terms of g factors (Hosemann & Bagchi, 1962). In the one-dimensional case, the integral width $w=(2\pi)^{1/2}\Delta$, where Δ is the root mean square value of the motion. The g factor is a ratio and is defined as $g=\Delta/d$, where d is the average repeat unit of the lattice.

Helical systems

In the three-dimensional case $\mathbf{r}$ has Cartesian coordinates x, y, z in real space while $\mathbf{R}$ has reciprocal-space coordinates X, Y, Z. Cylindrical coordinates are used in helical diffraction: $\mathbf{r}$ has coordinates ρ, φ, z while $\mathbf{R}$ has coordinates ξ, Φ, Z. The magnitudes r and R have the property that $r^2=\rho^2+z^2$ and $R^2=\xi^2+Z^2$ respectively. The diffracted intensity from a helix is denoted $I(\xi, \Phi, Z)$. In a diffraction experiment, the cylindrically averaged intensity $I(\xi, Z)$ is recorded, where

$$I(\xi, Z)=(1/2\pi)\int_0^{2\pi} I(\xi, \Phi, Z)\,\mathrm{d}\Phi. \qquad (16)$$

Thus, in order to compare with experiment, we need to obtain an expression for $I(\xi, Z)$.

By analogy with the one-dimensional case we first need to define the lattice-generating function $\psi(\mathbf{r})$ for the helix and hence obtain an expression for the a.c.f. $l(\mathbf{r})$ for the helix. In this section we consider only elementary helices which contain point atoms. Since point atoms can conveniently be represented by a unit-weight delta function, and, as the Fourier transform of a delta function is unity, from (4) it follows that the diffracted intensity $I(\xi, Z)$ for this elementary helix is the same as the averaged interference function $L(\xi, Z)$. We consider the undistorted helix, and then special helices with well defined lattice disorders.

No disorder

This perfect helix contains a total of S lattice points. It has M subunits (point atoms) in N turns with radius r_0, subunit repeat h and pitch p. The helix repeat is c and $c=Mh=Np$. From (5) the lattice-generating function $\psi(\mathbf{r})$ for this helix can be expressed in series form as

$$\psi(\mathbf{r})=\sum_{j=0}^{j=S-1}\delta(\rho-r_0, \varphi-j\varphi_0, z-jh), \qquad (17)$$

where the $j=0$ (the origin point) of the helix has coordinates $r_0, 0, 0$. Since $M\varphi_0=N2\pi$ the value of φ_0 is specified: $\varphi_0=2\pi N/M$. It is convenient to use the notation $\varphi_0=2\varepsilon$, where $\varepsilon=\pi N/M$. The a.c.f. $l(\mathbf{r})$ for the helix follows from (2) after changing variables. $l(\mathbf{r})$ in series form is expressed as

$$l(\mathbf{r})=S\delta(\mathbf{r}-0)+\sum_{m=1}^{m=S-1}(S-m)\delta(\mathbf{r}+\mathbf{r}_m), \qquad (18)$$

where the delta functions at $\mathbf{r}_m$ have coordinates $\Delta_m, \varphi_m, \pm mh$. The value of the radius Δ_m is given by

$$\Delta_m=2r_0|\sin m\varepsilon|. \qquad (19)$$

The a.c.f. $l(\mathbf{r})$ for this perfect helix consists of a series of delta functions on rings of radius Δ_m in planes at right angles to the z axis and with intercepts $z=\pm mh$. The first delta function on the ring of radius Δ_m has φ coordinate $\varphi_m=\pi/2+m\varepsilon$. Each ring contains $S-m$ delta functions uniformly distributed on the ring with angular separation $m\varphi_0$. All delta functions lie on the z axis ($\Delta_m=0$) when $m=0, \pm M, \pm 2M, \pm 3M$ *etc.* The a.c.f. $l(\mathbf{r})$ becomes $l(\rho, z)$ on rotation about the z axis. A drawing of the cylindrically symmetric a.c.f. $l(\rho, z)$ for this perfect helix is shown in Fig. 1.

The relationship between the a.c.f. $l(\rho, z)$ and the cylindrically symmetric Patterson function of the helix is noted. A plane section through $l(\rho, z)$ containing the z axis shows discrete delta-function peaks at radii Δ_m and at levels of $z=mh$. This plane section corresponds to the Patterson function of the elementary helix.

The Fourier transform of the a.c.f. $l(\mathbf{r})$ is $L(\mathbf{R})$, where $l(\mathbf{r})\Leftrightarrow L(\mathbf{R})$. For comparison with experiment,

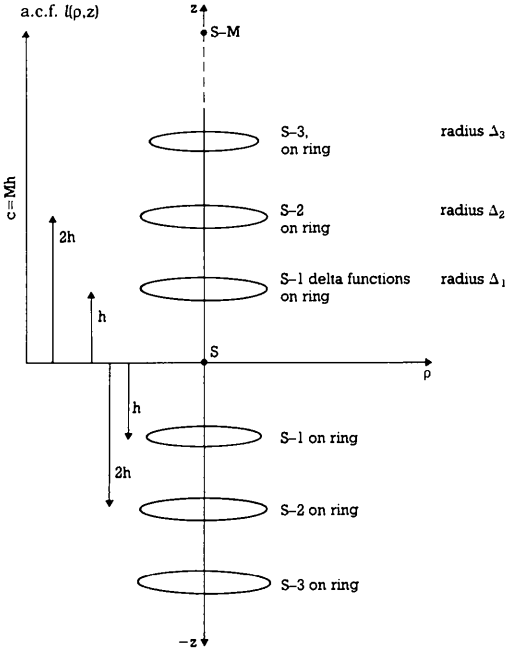

Fig. 1. A diagram of the a.c.f. $l(\rho, z)$ for the perfect helix. The rings in the planes $z=\pm mh$ are shown as continuous lines. The mth ring contains $S-m$ delta functions uniformly distributed on a circle of radius Δ_m. All delta functions are confined to the z axis when $m=0, \pm M, \pm 2M, \pm 3M$ *etc.*

the cylindrically averaged interference function $L(\xi, Z)$ as defined in (16) is required. When $\xi = 0$ the interference function $L(\xi, Z)$ reduces to $L(0, Z)$: note that $L(0, Z)$ has the same form as (7). The helical diffraction pattern has discrete layer lines which occur when $Z = lC$, where l is an integer and where $C = 1/c$. Thus, the averaged interference function becomes $L(\xi, l)$.

The Fourier-transform contribution due to each delta function on the ring of radius Δ_m is $\exp[-i2\pi\xi\Delta_m \cos(\varphi_m - \Phi)]$. After cylindrically averaging over Φ as defined by (16) a single term $J_0(2\pi\xi\Delta_m)$ is obtained (James, 1962). The interference function $L(\xi, l)$ for the helix is then given by

$$L(\xi, l) = S + 2 \sum_{m=1}^{m=S-1} (S-m) J_0(2\pi\xi\Delta_m) \cos 2\pi ml/M, \tag{20}$$

where Δ_m is defined by (19).

The diffracted intensity $I(\xi, l)$ for this elementary helix is equal to $L(\xi, l)$. At first sight, (20) looks inadequate to account for the characteristic layer-line profiles. Nevertheless, computer calculations readily demonstrate that (20) gives the correct layer-line profiles. It will be shown that (20) is, in fact, identical to the classical formula for helical diffraction. This follows from an expansion for $J_0(2\pi\xi\Delta_m)$ containing Bessel functions of different orders (Jeffreys & Jeffreys, 1962).

Equation (20) for $L(\xi, l)$ has a certain simplicity, since it contains only zero-order Bessel functions and cosine terms. On the other hand, the summation is over $\pm S$ terms (this includes the origin term and $\pm S - 1$ terms) with different weight factors $S - m$, so that the end result is not intuitively obvious. In the case of the perfect helix, it will be shown that the summation can be simplified by summing over M terms with equal weight factors (w).

This result follows from the study of 'matched pairs' which have the same $J_0(2\pi\xi\Delta_m)$ coefficients. The helix has M subunits in N turns and μ repeat units such that $S = \mu M$. There are E 'matched pairs' within each repeat unit: $E = (M-1)/2$, M is odd while $E = (M-2)/2$, M is even. The first 'matched pair' has coefficient $J_0(2\pi\xi\Delta_1)$ and occurs when $m = 1$ and $m = M - 1$ within the first repeat unit [of the summation in (20)]. The jth 'matched pair' with the same coefficient $J_0(2\pi\xi\Delta_j)$ within the kth repeat unit, has a combined weight factor of $2S - (2k-1)M$, where $1 \le j \le E$ and $1 \le k \le \mu$ and where j and k are integers. The sum of the weight factors for each of the μ 'matched pairs' is

$$2 \sum_{k=1}^{\mu} [2S - (2k-1)M].$$

This sum is equal to $2\mu S$. As the desired summation is over M terms, we now assign weight factor $w \times \mu S$ to each of the two terms contained within the 'matched pairs'. There is the origin term to consider: this is the $m = M$ term of the summation. It contains the single terms corresponding to $m = 0, \pm M, \pm 2M, \ldots \pm(\mu - 1)M$. The weight factor for the jth single term within the kth repeat is $S - kM$. The sum of the weight factors for the $m = 0$ and the $2(\mu - 1)$ single terms is

$$S + 2 \sum_{k=1}^{\mu-1} [S - kM].$$

This sum is $w = \mu S$. When M is even, there is also the $m = M/2$ term to consider. Similarly, it can be shown that the weight factor for this term is

$$2 \sum_{k=1}^{\mu} (kM - M/2).$$

This sum is $w = \mu S$.

Finally, the cylindrically averaged intensity $I(\xi, l)$ can be expressed as a summation over M terms and, since all terms in the new summation have the same weight factor $w = \mu S$, we can write

$$I(\xi, l) = \mu S \sum_{m=1}^{m=M} J_0(2\pi\xi\Delta_m) \cos 2\pi ml/M. \tag{21}$$

A plot of the diffracted intensity $I(\xi, l)$ for the actin helix is shown in Fig. 2. The intensities were computed using (21). Model parameters are $M = 15$, $N = 7$, $c = 410$ and $r_0 = 40$ Å (Worthington, 1959) and $\mu = 6$. These parameters refer to an early model and, although the modern parameters are different (Tajima, Kamiya & Seto, 1983), the calculation makes the point required. The only difference between the earlier and the modern parameters is in the numbering

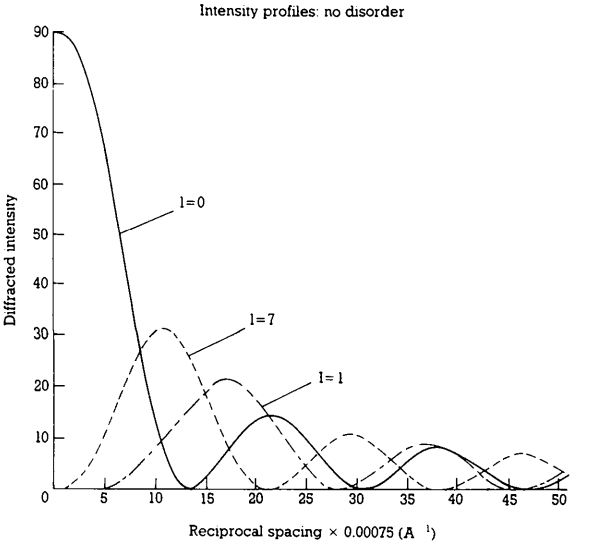

Fig. 2. The diffracted intensity $I(\xi, l)$ for the actin helix showing layer lines $l = 0$, $l = 1$ and $l = 7$. The intensities were calculated using equation (21) and model parameters $M = 15$, $N = 7$, $c = 410$ and $r_0 = 40$ Å with $\mu = 6$; see text.

of the layer lines. The layer-line intensity profiles are unaltered. The layer-line intensities $I(\xi, l)$ for $l=0$, $l=1$ and $l=7$ are shown. The $l=0$, $l=7$ and $l=1$ curves are readily identified as the classical $J_0^2(\ )$, $J_1^2(\ )$ and $J_2^2(\ )$ profiles. In Fig. 2 the value of $S=\mu M$ is fixed by our choice of $\mu=6$. If μ is larger then the width of the layer-line profiles along the Z axis becomes sharper: the integral width of the profile along the Z axis is proportional to $1/S$ (James, 1962). Provided that $\mu>1$ and that μ is an integer, the value of S will not affect the diffracted intensity profiles of the layer lines in the radial direction (ξ).

The condensed formula (21) for $i(\xi, l)$ provides a convenient starting point for demonstrating the equivalence of our equation (20) to the classical formulas of helical diffraction. The expansion (Jeffreys & Jeffreys, 1962) for $J_0(2\pi\xi\Delta_m)$ is

$$J_0(2\pi\xi\Delta_m)=\sum_{n=-\infty}^{n=\infty} J_n^2(2\pi\xi r_0)\cos nm\varphi_0, \quad (22)$$

where n is an integer and where $m\varphi_0=m2\pi N/M$ is the angle subtended by Δ_m at the centre of the elementary helix of radius r_0. On substituting (22) into (21), and, for a specific value of n, we obtain

$$I(\xi, l)=\mu S J_n^2(2\pi\xi r_0)\Omega(n, l), \quad (23)$$

where $\Omega(n, l)$ is the sum of the product of cosines:

$$\Omega(n, l)=\sum_{m=1}^{m=M} \cos 2\pi mNn/M \cos 2\pi ml/M. \quad (24)$$

By expanding the product of the two cosines it can readily be shown that the factor $\Omega(n, l)=M$ when

$$l=Nn+Mv, \quad (25)$$

where n, v are integers, and that otherwise $\Omega(n, l)=0$. Equation (25) is the well known selection rule for helical diffraction. For example, if we choose $M=15$ and $N=7$ as the model parameters for the actin helix (Worthington, 1959) then the diffracted intensity on layer line $l=7$ is $I(\xi, 7)=S^2J_1^2(2\pi\xi r_0)$ in agreement with classical theory.

The effects of disorder on helical diffraction

In the general case the disorder is generated by three separate Gaussian functions which relate to the radius r_0, the axial angular displacement φ_0 and the subunit distance h. Radial disorder $b(r_0)$ is the r_0 variation, axial disorder $a(\varphi_0)$ is the φ variation while translational disorder $s(h)$ is the z variation. The combined Gaussian function expressing the location of each lattice point is $[b(r_0)*a(\varphi_0)]s(h)$, where the three Gaussian functions have integral widths u, v, w respectively. It is convenient to write $c(\rho, \varphi)=[b(r_0)*a(\varphi_0)]$. In general, the Gaussian probability $c(\rho, \varphi)$ is not cylindrically symmetric, that is, $c(\rho, \varphi)\neq c(\rho)$. The Fourier transform of $c(\rho, \varphi)$ is $C(\xi, \Phi)$, where $c(\rho, \varphi)\Leftrightarrow C(\xi, \Phi)$, and $C(\xi, \Phi)$ is also not cylindrically symmetric.

(1) *Special case of disorder with cylindrical symmetry*

The treatment of disorder is relatively straightforward when the cylindrically symmetric Gaussian function $c(\rho)$ is involved. In the case of no disorder, the Fourier transform contribution due to each delta function on the ring of radius Δ_m is $\cos[2\pi\xi\Delta_m\cos(\varphi_m-\Phi)]$ (we can ignore the sine contribution, the imaginary part, in this case because it disappears in the cylindrical averaging). After averaging over Φ the zero-order Bessel function $J_0(2\pi\xi\Delta_m)$ is obtained. In the special case when the cylindrically symmetric Gaussian function $c(\rho)$ is involved the $J_0(2\pi\xi\Delta_m)$ function is again obtained but multiplied by the appropriate Fourier transform.

It is convenient to consider thermal and paracrystalline disorder in parallel. In the one-dimensional case the interference functions for thermal disorder, defined by (12), and paracrystalline disorder, defined by (15), differ only in the exponents of the Gaussian transforms e^{-2M} and $Q^m(X)$, that is, 2 for thermal and m for paracrystalline. Recall that thermal disorder refers to variation about each lattice point whereas paracrystalline disorder is cumulative with only average values for the model parameters r_0, φ_0, h.

We first treat the special case when $c(\rho, \varphi)=c(\rho)$, that is, when $g(r)$ has cylindrical symmetry about the helical axis (the z axis). The disorder probability is Gaussian and is represented by $g(r)$, where r is the magnitude of $\mathbf{r}$ in real space. The cylindrically symmetric Gaussian function $g(r)$ can be expressed as a product of two Gaussians: $g(r)=c(\rho)s(z)$, where $s(z)$ has the same form as (8). The cylindrically symmetric Gaussian function $c(\rho)$ is given by

$$c(\rho)=(1/u)^2\exp[-\pi(\rho/u)^2], \quad (26)$$

where u is the integral width. The Fourier transforms of $g(r)$, $c(\rho)$ and $s(z)$ are $G(R)$, $C(\xi)$ and $S(Z)$ respectively. Since $g(r)\Leftrightarrow G(R)$, it follows that $G(R)=C(\xi)S(Z)$. By analogy with the one-dimensional case, we can write $G(R)=e^{-B}$, where $B=\mathcal{U}+\mathcal{W}$: $\mathcal{U}=\pi(u\xi)^2$ and $\mathcal{W}=\pi(wz)^2$.

The a.c.f. of the cylindrically symmetric disordered elementary helix is $l_{cs}(\mathbf{r})$ and from (11) and (18) it follows that

$$l_{cs}(\mathbf{r})=S\delta(\mathbf{r}-0)+\sum_{m=1}^{m=S-1}(S-m)\delta(\mathbf{r}+\mathbf{r}_m)*\tilde{g}^t(r), \quad (27)$$

where the delta functions at $\mathbf{r}_m$ have cylindrical coordinates Δ_m, φ_m, $\pm mh$ and where $t=2$ for thermal disorder and $t=m$ for paracrystalline disorder. By analogy with the one-dimensional case, the Fourier transform of $\tilde{g}^t(r)$ is e^{-tB}. The Fourier transform of $l_{cs}(\mathbf{r})$ is $L_{cs}(\mathbf{R})$, where $l_{cs}(\mathbf{r})\Leftrightarrow L_{cs}(\mathbf{R})$. In order to compare with experiment, we require $L_{cs}(\xi, l)$, the

cylindrically averaged interference function, and, on modifying (20), we obtain

$$L_{cs}(\xi, l) = S + 2 \sum_{m=1}^{m=S-1} e^{-tB}(S-m) J_0(2\pi\xi\Delta_m) \times \cos 2\pi ml/M. \quad (28)$$

The averaged diffracted intensity $I_{cs}(\xi, l)$ is also given by (28) as point atoms are involved.

In case of thermal disorder, when $t = 2$, the diffracted intensity $I_{td}(\xi, l)$ from the cylindrically symmetric disordered helix can be expressed in two parts similar to (13). Thus, $I_{td}(\xi, l)$ in this form is given by

$$I_{td}(\xi, l) = S[1 - e^{-2B}] + e^{-2B} I(\xi, l). \quad (29)$$

In the case of paracrystalline disorder, when $t = m$, the diffracted intensity $I_{pd}(\xi, l)$ from the cylindrically symmetric disordered helix is given by

$$I_{pd}(\xi, l) = S + 2 \sum_{m=1}^{m=S-1} (S-m) J_0(2\pi\xi\Delta_m)\, e^{-mB} \times \cos 2\pi ml/M, \quad (30)$$

where e^{-mB} is the Fourier transform of $\tilde{q}^m(r)$ and where $B = \mathcal{U} + \mathcal{W}$: $\mathcal{U} = \pi(u\xi)^2$ and $\mathcal{W} = \pi(wl/M)^2$. From (30), when only paracrystalline disorder $c(\rho)$ is involved, the fall-off in intensity is a function of ξ only and is the same for all layer lines.

A plot of the diffracted intensity $I_{pd}(\xi, l)$ for the actin helix is shown in Fig. 3. The intensities were computed using (30) and the same model parameters as in Fig. 2. Only Gaussian disorder $c(\rho)$ in a plane at right angles to the helical axis is considered. The layer-line profiles are $l = 0$ and $l = 7$: the continuous curves have no disorder while the dotted curves have paracrystalline disorder with $g = 0{\cdot}057$, where g is expressed as a fraction of r_0. From Fig. 3 the fall-off in intensity due to paracrystalline disorder $c(\rho)$ is a function of ξ only, in agreement with theory.

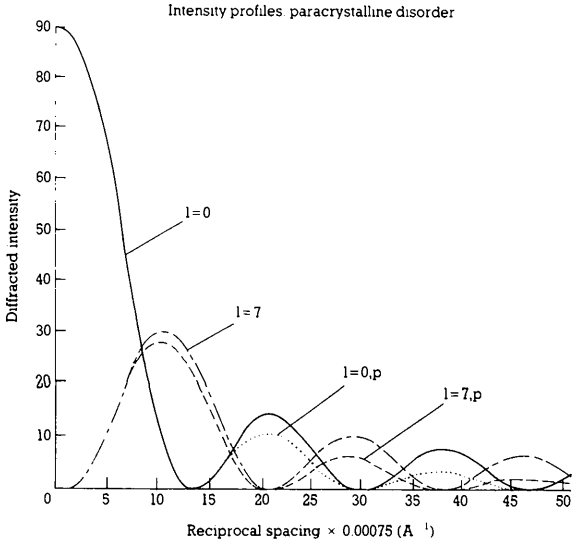

Fig. 3. Diffracted intensity profiles $I_{pd}(\xi, l)$ for the actin helix with paracrystalline disorder. Only Gaussian disorder $c(\rho)$ is considered. The intensities for layer lines $l = 0$ and $l = 7$ were computed using equation (30) and the same model parameters as in Fig. 2. The continuous curves have no disorder while the dotted curves have paracrystalline disorder with $g = 0{\cdot}057$.

(2) *General case of disorder with no symmetry*

In the general case when the non-symmetric Gaussian probability $c(\rho, \varphi)$ is involved, the averaging process is complicated in that the appropriate Fourier transform associated with $c(\rho, \varphi)$ has to be included into the averaging process. Consequently an explicit result has not been obtained. The mathematical expressions can, however, be set up on a computer.

It is convenient first to consider axial disorder $a(\varphi_0)$ and radial disorder $b(r_0)$ separately. When only one disorder is present then $c(\rho, \varphi)$ is one-dimensional, that is, $c(\rho, \varphi) = c(\boldsymbol{\rho})$. The Fourier transform of $c(\boldsymbol{\rho})$ is $C(\boldsymbol{\xi})$ and both functions have the same orientation θ_m. Recall that the delta function at $\mathbf{r} = \mathbf{r}_m$ has orientation φ_m. When the Fourier transform is included in the averaging process, it is the difference in φ values which is relevant. The difference is denoted ε_m and $\varepsilon_m = \theta_m - \varphi_m$.

In the general case of disorder, when the non-symmetric Gaussian function $c(\rho, \varphi)$ is involved, the appropriate Fourier transform to be included in the averaging process is $C^t(\xi, \Phi)$, where $t = 2$ for thermal disorder and $t = m$ for paracrystalline disorder. In the special case when $c(\rho, \varphi)$ is a one-dimensional function, the cylindrically averaged contribution for this single disorder is denoted $D_m(\xi)$ and, in integral form, $D_m(\xi)$ is

$$D_m(\xi) = (1/2\pi) \int_0^{2\pi} \cos(2\pi\xi\Delta_m \cos\Phi) \times C^t[\xi \cos(\Phi + \varepsilon_m)]\, d\Phi. \quad (31)$$

Equation (31) is derived by choosing $\Phi = \varphi_m$ as the origin for the Φ sampling as Φ varies from 0 to 2π. $D_m(\xi)$ can also be expressed in series form as

$$D_m(\xi) = (1/J) \sum_{j=0}^{j=J-1} \cos[2\pi\xi\Delta_m \cos\omega_j] \times C^t[\xi \cos(\omega_j + \varepsilon_m)], \quad (32)$$

where $\omega_j = j2\pi/J$. The value of J is chosen large enough to give correct sampling. Since each delta function on the ring of radius Δ_m has the same difference in orientation ε_m it follows that (32) is valid for each of the $S - m$ delta functions.

The cylindrically averaged interference function for the disordered helix with one-dimensional disorder $c(\boldsymbol{\rho})$ and translational disorder $s(z)$ is denoted

$L_{od}(\xi, l)$ and is given by

$$L_{od}(\xi, l) = S + 2 \sum_{m=1}^{m=S-1} \exp(-t\mathcal{W}) \times (S-m) D_m(\xi) \cos 2\pi ml/M, \quad (33)$$

where $\mathcal{W} = \pi(wl/Mh)^2$. Note that (33) has been derived for the case of a single disorder when $c(\rho, \varphi)$ becomes a one-dimensional function. Equation (33) is also valid for the case of two disorders provided that the factor $D_m(\xi)$ is modified.

(*A*) *Axial disorder.* Axial disorder refers to the φ variation centred on the average value φ_0. This variation is expressed in terms of tangential motion relative to the helical axis. The one-dimensional Gaussian function for axial disorder is $a(\varphi_0)$ and, therefore, $a(\varphi_0) = a(\mathbf{\rho})$. The Gaussian function $a(\mathbf{\rho})$ has the same form as (8) but with integral width $v = (2\pi)^{1/2} r_0 \delta\varphi$. The Fourier transform of $a(\mathbf{\rho})$ is $A(\xi)$ and both transforms have the same orientation θ_m, where $\theta_m = \pi/2 + 2m\varepsilon$. Since $\varphi_m = \pi/2 + m\varepsilon$, the difference $\varepsilon_m = \theta_m - \varphi_m$ is $\varepsilon_m = m\varepsilon$. The factor $D_m(\xi)$ for axial disorder is expressed in series form as in (32) when the appropriate Fourier transform $C'(\xi, \Phi)$ is given by

$$C'(\xi, \Phi) = \exp\{-t\pi[v\xi \cos(\omega_j + m\varepsilon)]^2\}. \quad (34)$$

The $\cos^2 m\varepsilon$ term which appears in the exponential part of (34) can be identified with the size of the rings in the a.c.f. $l(\rho, z)$ for the helix. Since the radius Δ_m is defined by (19), we can write

$$\cos^2 m\varepsilon = 1 - (\Delta_m/2r_0)^2. \quad (35)$$

Thus, the $\cos^2$ term is zero when $\Delta_m = 2r_0$ and unity when $\Delta_m = 0$. In general, the radius Δ_m varies between 0 and $2r_0$ and, therefore, axial disorder will modify the values of the factors $D_m(\xi)$.

The effect of axial disorder in the thermal and paracrystalline modes is similar. Differences are expressed by the factors $D_m(\xi)$ as defined by (32). We choose to examine the paracrystalline mode. The averaged intensity $I_{pd}(\xi, l)$ for axial disorder was computed using (32), (33) and (34). The intensities for layer lines $l = 7$ and $l = 1$ of the actin helix are shown in Figs. 4(*a*) and (*b*) respectively. The model parameters for the actin helix are the same as in Figs. 2 and 3. The axial disorder $(a, 0, 0)$ profiles have $g = 0{\cdot}04$. In Fig. 4(*a*) the $l = 7$ profile with axial disorder $(a, 0, 0)$ is only marginally reduced in intensity whereas in (*b*) the $l = 1$ profile with axial disorder $(a, 0, 0)$ is noticeably reduced in intensity compared with the profile without disorder $(0, 0, 0)$.

(*B*) *Radial disorder.* Radial disorder refers to the r_0 variation when the lattice point of the helix has variation along the radius directed towards r_0. The one-dimensional Gaussian function $b(\mathbf{\rho})$ describes the variation about r_0. The Gaussian function $b(\mathbf{\rho})$ has the same form as (8) but with integral width $u = (2\pi)^{1/2}\delta r$. The orientation of $b(\mathbf{\rho})$ relative to $a(\mathbf{\rho})$ is fixed at right angles. The Fourier transform of $b(\mathbf{\rho})$ is $B(\xi)$; $B(\xi)$ is also one-dimensional and it has the same form as (9). Since $b(\mathbf{\rho})$ and $B(\xi)$ have orientation $\theta_m = 2m\varepsilon$, the difference $\varepsilon_m = \theta_m - \varphi_m$ is given by $\varepsilon_m = m\varepsilon - \pi/2$. Thus, the $\cos(\Phi + \varepsilon_m)$ term in (31)

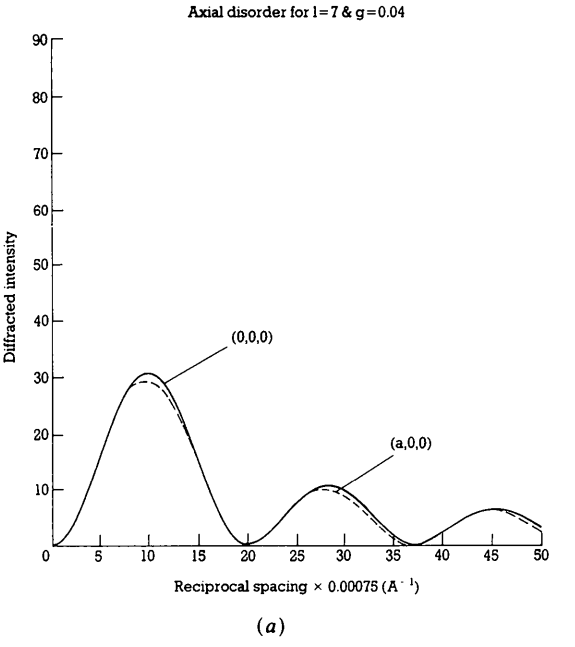

(*a*)

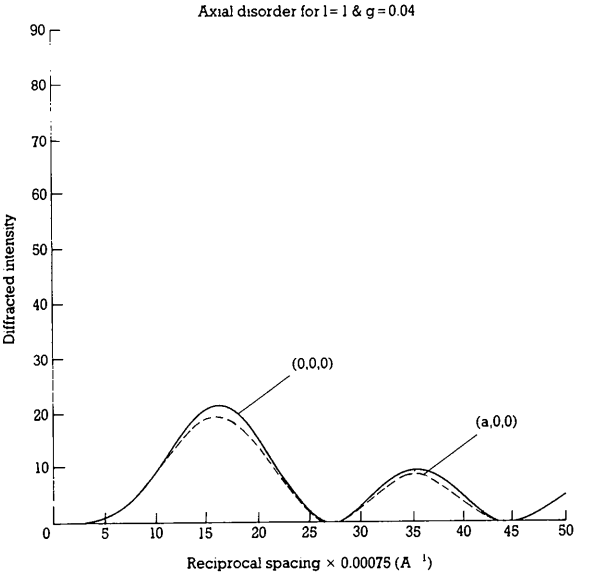

(*b*)

Fig. 4. Diffracted intensity profiles $I_{pd}(\xi, l)$ for the actin helix with the same model parameters as in Figs. 2 and 3. The intensities for layer lines $l = 7$ and $l = 1$ are shown in (*a*) and (*b*) respectively. The axial-disorder $(a, 0, 0)$ profiles (dotted lines) have $g = 0{\cdot}04$. The $(0, 0, 0)$ profiles (continuous lines) have no disorder.

becomes $\sin(\Phi + m\varepsilon)$. The appropriate Fourier transform $C^t(\xi, \Phi)$ in (32) then becomes

$$C^t(\xi, \Phi) = \exp\{-t\pi[u\xi \sin(\omega_j + m\varepsilon)]^2\}. \quad (36)$$

We choose to examine the effect of radial disorder in the paracrystalline mode. The averaged intensity $I_{pd}(\xi, l)$ for radial disorder was computed using (32), (33) and (36). The intensities for layer lines $l = 7$ and $l = 1$ of the actin helix with the same model parameters as before are shown in Figs. 5(a) and (b) respectively. The two radial disorder (0, b, 0) profiles have $g = 0{\cdot}04$ and are both noticeably reduced in intensity compared with the (0, 0, 0) profiles without disorder.

(*C*) *Axial and radial disorder.* When axial and radial disorder occur together the appropriate Fourier transform $C^2(\xi, \Phi)$ is given by the product of the two transforms in (34) and (36). By writing $A = (\pi r_0 g_\varphi \xi)^2$, where $g_\varphi = \delta\varphi$, and $R = (\pi r_0 g_r \xi)^2$, where $g_r = \delta r$, the combined Fourier transform $C^t(\xi, \Phi)$ becomes

$$C^t(\xi, \Phi) = \exp[-t(A+R)] \times \exp[-t(A-R)\cos 2(\omega_j + m\varepsilon)]. \quad (37)$$

In the special case when the axial and radial disorders are equal, that is, when $A = R$, the Fourier transform $C^t(\xi, \Phi)$ is cylindrically symmetric and is given by $\exp(-2tA)$. In the thermal mode, the Gaussian transform $\exp(-2\mathcal{U})$ from (30) is equal to e^{-4A} while, in the paracrystalline mode, the Gaussian transform $\exp(-m\mathcal{U})$ is equal to e^{-2mA}.

As previously, we choose to examine the paracrystalline mode. The averaged intensity $I_{pd}(\xi, l)$ for axial and radial disorder was computed using (32), (33) and (37). The layer-line intensities $l = 7$ and $l = 1$ for the actin helix with the same parameters as before are shown in Figs. 6(a) and (b) respectively. Both (a, b, 0) profiles have equal axial and radial disorder: $g_\varphi = 0{\cdot}04$ and $g_r = 0{\cdot}04$. The (a, b, 0) profile for $l = 7$ in Fig. 6(a) is the same as the $l = 7$ profile with paracrystalline disorder $g = 0{\cdot}057$ in Fig. 3.

(*D*) *Translational disorder.* The inclusion of translational disorder is straightforward: it follows directly from the one-dimensional case. The Gaussian probability expressing the z variation is $s(z)$ with integral width w. The Fourier transform of $s(z)$ is $S(Z) = \exp(-\mathcal{W})$, where $\mathcal{W} = \pi(wZ)^2$. We treat the case of translational disorder only, that is, $s(z)$ is finite but with $c(\rho, \varphi) = 0$. The diffracted intensity for a simple helix with translational disorder is denoted $I_z(\xi, l)$ and, from (28), is given by

$$I_z(\xi, l) = S + 2\sum_{m=1}^{m=S-1} \exp(-t\mathcal{W})(S-m)J_0(2\pi\xi\Delta_m) \times \cos 2\pi ml/M, \quad (38)$$

where $t = 2$ for thermal disorder and $t = m$ for paracrystalline disorder.

As previously, we choose to examine translational disorder in the paracrystalline mode. The integral width w is chosen to have the same amount of disorder as in Fig. 3, so that the corresponding g value is 0·0585. Computer simulation of $I_{pd}(0, l)$ for the actin helix with the same model parameters as before shows a series of delta-function-like peaks at $l = 0, \pm 15, \pm 30,$

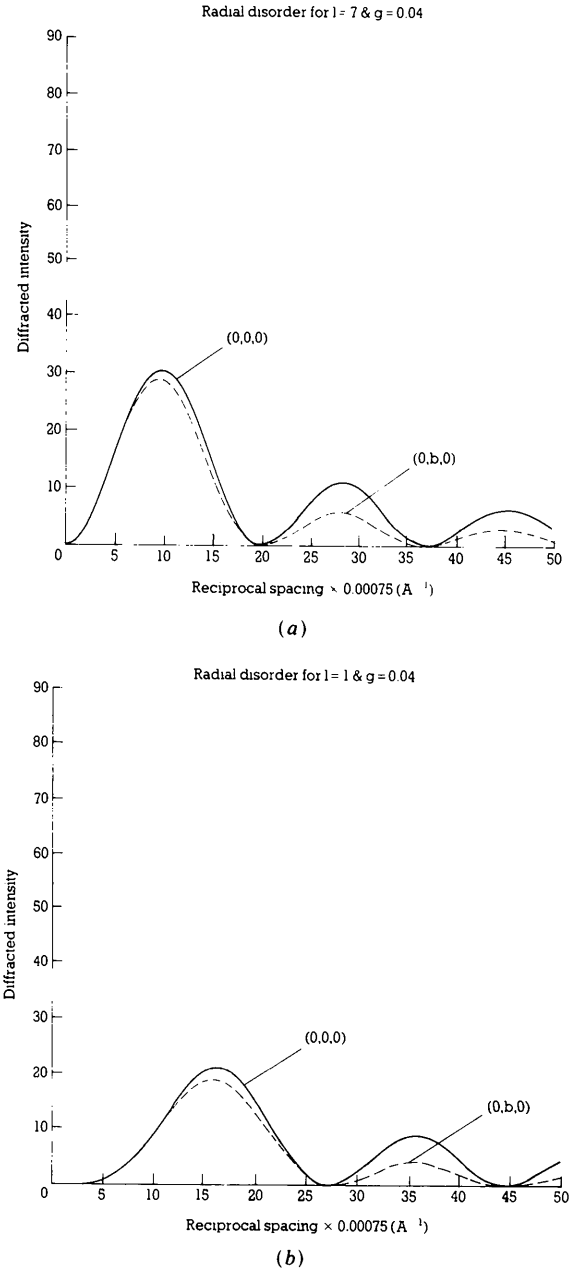

Fig. 5. Diffracted intensity profiles $I_{pd}(\xi, l)$ for the actin helix with the same model parameters as in Figs. 2 and 3. The intensities for layer lines $l = 7$ and $l = 1$ are shown in (a) and (b) respectively. The radial-disorder (0, b, 0) profiles (dotted lines) have $g = 0{\cdot}04$. The (0, 0, 0) profiles (continuous lines) have no disorder.

±45 *etc.* It is not worthwhile to show the resulting intensity plots since they are not informative. The integral widths of the peaks are very small; only the heights of the peaks are different. The first three meridional reflections from the actin helix with $g = 0{\cdot}0585$ when compared with the zero-order height of 1·0 have heights 0·94, 0·77 and 0·55 respectively.

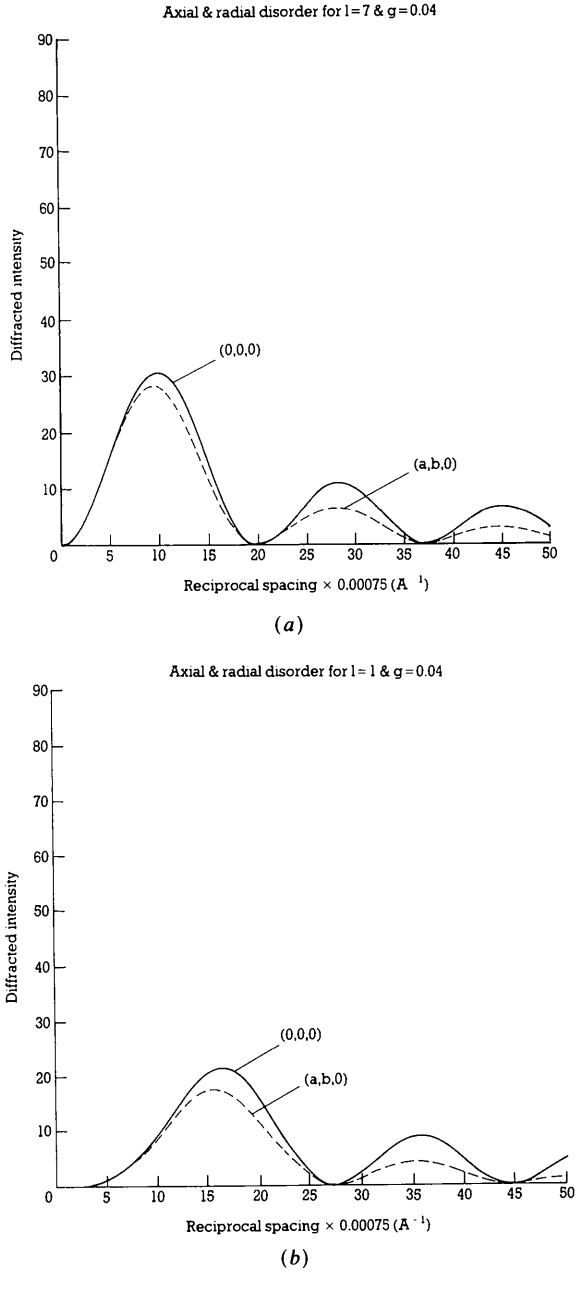

Fig. 6. Diffracted intensity profiles $I_{pd}(\xi, l)$ for the actin helix with same model parameters as in Figs. 2 and 3. The intensities for layer lines $l = 7$ and $l = 1$ are shown in (*a*) and (*b*) respectively. The two (*a*, *b*, 0) profiles (dotted lines) with axial and radial disorder have the same *g* value of 0·04. The (0, 0, 0) profiles (continuous lines) have no disorder.

Comparisons with previous work

The disorder due to axial, translational and screw displacements along the helical axis of chain molecules in a crystalline array has been previously studied and equations have been derived for these effects (Clark & Muus, 1962). Our treatment refers to disorder within the helix itself and is, therefore, not directly comparable. The formulas for axial and for translational disorder in the thermal mode are of interest, however. The formula for thermal translational disorder (Clark & Muus, 1962) is similar: it has the same Gaussian transform as we have obtained, that is, $\exp(-2\mathcal{W})$.

The study of thermal axial disorder (Clark & Muus, 1962) led to the often-quoted formula which, in our notation, is

$$I_{td}(\xi, l) = I(\xi, l) \exp[(n\delta\varphi)^2], \qquad (39)$$

where n is the order of the Bessel function and where the value of n is given by the selection rule (25). Our formulas (33) and (34) for axial disorder within the helix do not directly involve n, the order of the Bessel function. However, we can write for the maxima of each Bessel function $n \simeq k\xi$, where k is a constant. Thus, (39) becomes

$$I_{td}(\xi, l) \simeq I(\xi, l) \exp[-(k\delta\varphi\xi)^2], \qquad (40)$$

and the exponential factor in (40) is now similar to our Gaussian transform $\exp(-2\mathcal{U})$, where $\mathcal{U} = \pi(u\xi)^2$.

The angular motion of subunits in the actin helix has recently been studied by Egelman & DeRosier (1982). These authors derive an expression for the expectation value of the intensity $\langle I \rangle$ for the case of cumulative random angular motions of the subunits. In later work, this expression has been reformulated (Barakat, 1987) and, in our notation, is

$$\langle I_{pd}(m, l) \rangle = S \coth(n\delta\varphi/2)^2. \qquad (41)$$

Egelman & DeRosier (1982) treat the case when $(n\delta\varphi)^2 \ll 1$ so that $\langle I_{pd}(n, l) \rangle = 4S/(n\delta\varphi)^2$. Thus, the layer-line intensities are proportional to $1/n^2$, where n is the order of the Bessel function. Equation (41) should, in principle, be comparable to our equations (33) and (34) for axial disorder in the paracrystalline mode. These analyses (Engelman & DeRosier, 1982; Barakat, 1987) are based upon statistical theory and the method is quite different from our analysis, so that the two analyses are not readily comparable.

Our equations (33) and (34) for axial disorder involve the Gaussian transform $C'(\xi, l) = \exp[-\alpha(\xi\delta\varphi)^2]$, where α includes the missing factors from (34). The individual $D_m(\xi)$ factors of (31) will show a fall-off in values as ξ increases. The diffracted intensity $I_{pd}(\xi, l)$ is obtained by summing over m values of $D_m(\xi)$ according to (33). The question of whether $I_{pd}(\xi, l)$ for axial disorder is directly related

to the order (n) of the characteristic Bessel functions is not readily answered from a study of (33) and (34). We consider that (33) and (34) are correct: the order number n does not appear explicitly in these equations, however.

Computer simulation of $I_{pd}(\xi, l)$ in Figs. 4(a) and (b) show that axial disorder has little influence on layer line $l=7$, $n=1$, whereas it has a noticeable effect on layer line $l=1$, $n=2$. The case of $l=0$, $n=0$ (which is not shown) resembles the case of $l=7$, $n=1$ in that the $l=0$ profile is little changed by axial disorder. Thus, the diffracted intensity $I_{pd}(\xi, l)$ as defined by (33) and (34) tends to show that axial disorder is directly related to the order (n) of the characteristic Bessel functions. It might be thought that the M and N values play an important role as they define the value of the radius Δ_m. Recall that $D_m(\xi)$ values are insensitive to axial disorder when Δ_m approaches $2r_0$. However, the calculated $I_{pd}(\xi, 3)$ and $I_{pd}(\xi, 6)$ profiles for the collagen helix with parameters of $M=10$, $N=3$ and with the same amount of axial disorder are identical to those in Figs. 4(a) and (b) respectively, after allowing for the different r_0 parameters. Thus, the n dependence of axial disorder is inherent in the framework of (33) and (34).

This work was carried out while CRW was on sabbatical leave at the Open University Oxford Research Unit, partially funded by National Eye Institute grant number EY05405. We are grateful to the Director, Dr D. A. Blackburn, and other members of the staff of the Oxford Research Unit for their interest and for helping us with access to the Open University computer network.

References

BARAKAT, R. (1987). *Acta Cryst.* A**43**, 45-49.
CLARK, E. S. & MUUS, L. T. (1962). *Z. Kristallogr.* **117**, 108-118.
COCHRAN, W., CRICK, F. H. C. & VAND, V. (1952). *Acta Cryst.* **5**, 581-586.
EGELMAN, E. H. & DEROSIER, D. J. (1982). *Acta Cryst.* A**38**, 796-799.
HOSEMANN, R. & BAGCHI, S. N. (1962). *Direct Analysis of Diffraction by Matter.* Amsterdam: North-Holland.
JAMES, R. W. (1962). *The Crystalline State*, Vol. II. London: Bell.
JEFFREYS, H. & JEFFREYS, B. (1962). In *Methods of Mathematical Physics.* Cambridge Univ. Press.
TAJIMA, Y., KAMIYA, K. & SETO, T. (1983). *Biophys. J.* **43**, 335-343.
VAINSHTEIN, B. K. (1966). *Diffraction of X-rays by Chain Molecules.* Amsterdam: Elsevier.
WORTHINGTON, C. R. (1959). *J. Mol. Biol.* **1**, 398-401.
WORTHINGTON, C. R. (1986). *Biophys. J.* **49**, 98-101.
WORTHINGTON, C. R. (1987). In *Patterson and Pattersons*, edited by J. P. GLUSKER, B. K. PATTERSON & M. ROSSI, pp. 558-568. Oxford: Clarendon Press.

SHORT COMMUNICATIONS

Contributions intended for publication under this heading should be expressly so marked; they should not exceed about 1000 *words; they should be forwarded in the usual way to the appropriate Co-editor; they will be published as speedily as possible.*

Acta Cryst. (1989). A**45**, 654-656

Experimental phase effects and X-ray wavelengths. By BEN POST, JOHN DIMARCO and WALTER KISZENICK, *Physics Department, Polytechnic University, Brooklyn*, 11201 *New York, USA*

(*Received* 14 *December* 1988; *accepted* 21 *March* 1989)

Abstract

It is shown that Shen & Colella [*Acta Cryst.* (1986). A**42**, 533-538; *Nature* (*London*). (1987). **329**, 232-233; *Acta Cryst.* (1988). A**44**, 17-21] are in error in asserting that 'irrespective of instrumental resolution' asymmetric n-beam benzil interactions can be recorded only if incident-beam wavelengths equal to, or greater than, 3·5 Å are used. Such interactions are clearly displayed in our Cu $K\alpha_1$ and Cr $K\alpha_1$ n-beam patterns of organic crystals, such as benzil, and that useful phase information can be readily extracted from such data.

In recent publications, Shen & Colella (1986, 1987, 1988), referred to below as 'S&C', described difficulties they encountered in their efforts to record asymmetric interaction maxima in n-beam patterns of organic acentric benzil crystals. In discussing results obtained with Cu $K\alpha_1$ and Cr $K\alpha_1$ they state that 'so far we have not been able to see the asymmetric effects in the wings of the Renninger peaks.' Their negative results were attributed to the very small half-widths and asymmetries of the benzil maxima, and to inadequacies of the instrumentation then available to them, *i.e.* 'the resolution needed on the φ scale ($\simeq 1'$) is not normally available in standard laboratory experiments. The only way to achieve this kind of resolution is to use a beam from a synchrotron light source' (Shen & Colella, 1986, p. 537).

We are aware of the many advantages of synchrotron X-ray sources over conventional ones. Clearly, they can

0108-7673/89/090654-03$03.00